

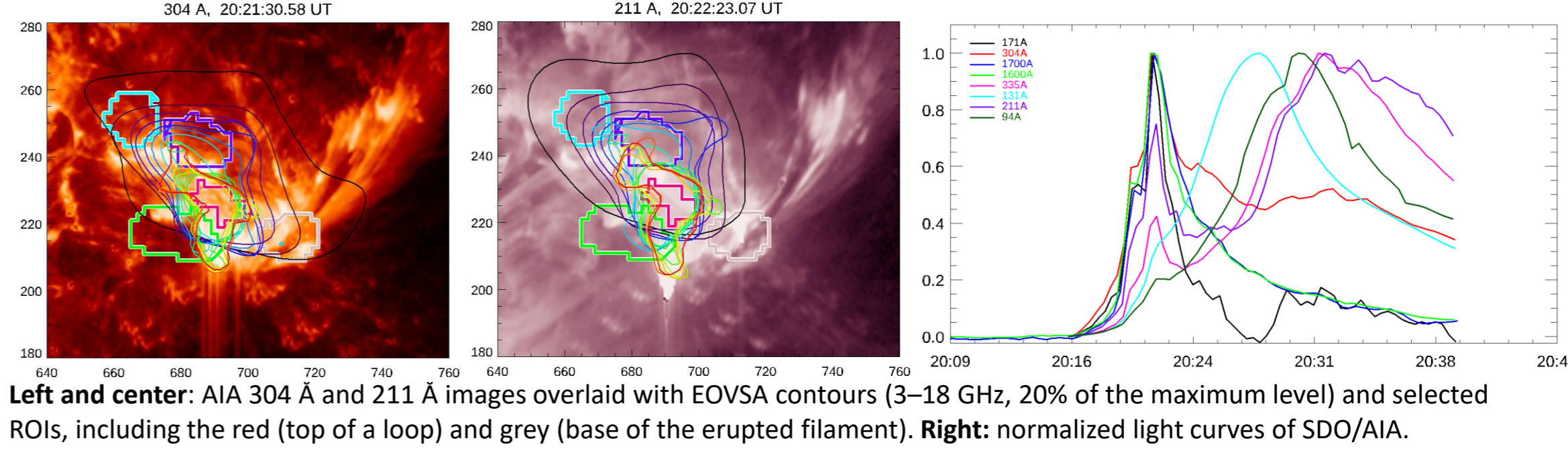
Locating sites of magnetic energy release in the 2022-10-02 X-class flare



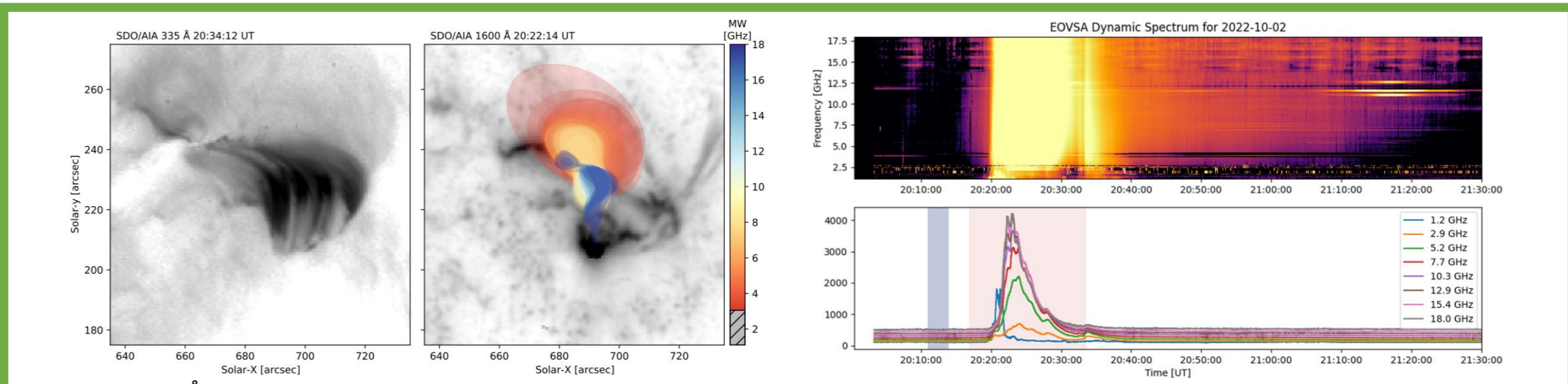
EOVSA's (Gary et al. 2018) 13-antenna design (78 unique baselines) enables successful measurements of magnetic fields and plasma properties in flares. EOVSA features imaging from 1–18 GHz at 1 s cadence, which is ideal for studying incoherent GS emission from flares. ~1.5 km maximum baseline limits its spatial resolution to ~50 arcsec/v[GHz].

Solar flares are driven by the release of free magnetic energy and are often associated with restructurization of the magnetic field topology. Observations of the evolving magnetic field in the flaring volume are limited to only one case, the X8.2 limb flare on 2017-09-10, where a coherent decay of the magnetic field in the corona was detected cospatial with efficient particle acceleration site at a cusp region. It remains unclear if this phenomenon is typical or exceptional. Here, we report another strong solar flare observed on the solar disk, whose microwave data permit mapping the magnetic field over the flaring source and tracking the magnetic field evolution over the course of the flare. This is done by model spectral fitting of the microwave imaging spectroscopy data obtained with NJIT's Expanded Owens Valley Array (EOVSA). The EOVSA images employed in this study were synthesized with overlapping 4 s time intervals and 2 s cadence at many frequencies between 2.5 and 18 GHz during the rise, peak, and early decay phases of the flare. The plasma parameters derived from this fitting display magnetic field decay in the loop top with the decay rate up to 10 G/s and in other locations.

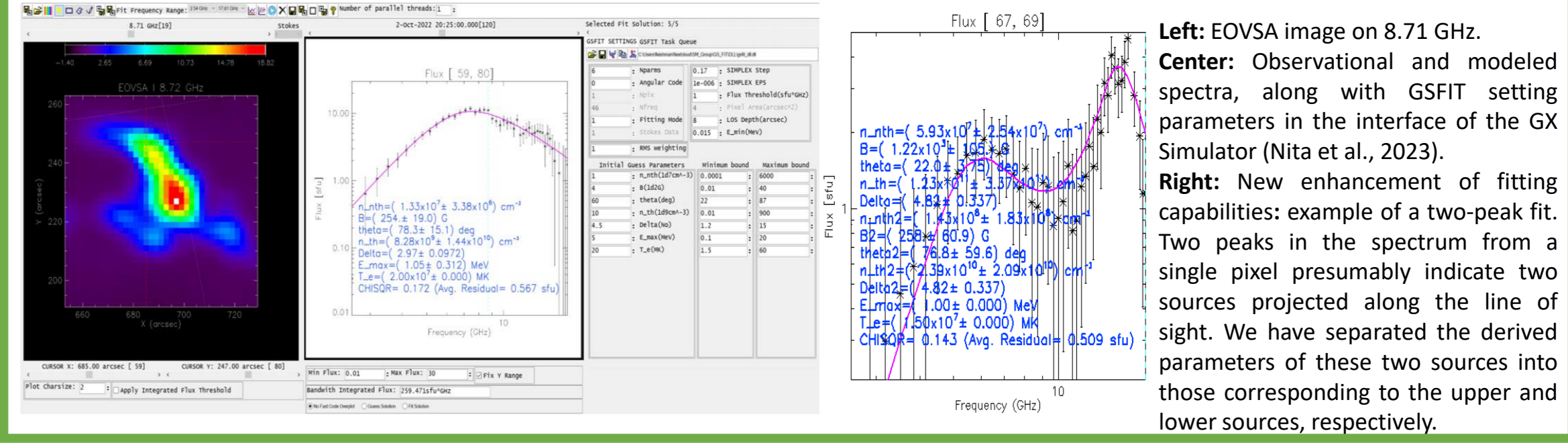
The X1.0 flare started at 19:53 UT and peaked at 20:25 UT on 2022 October 2



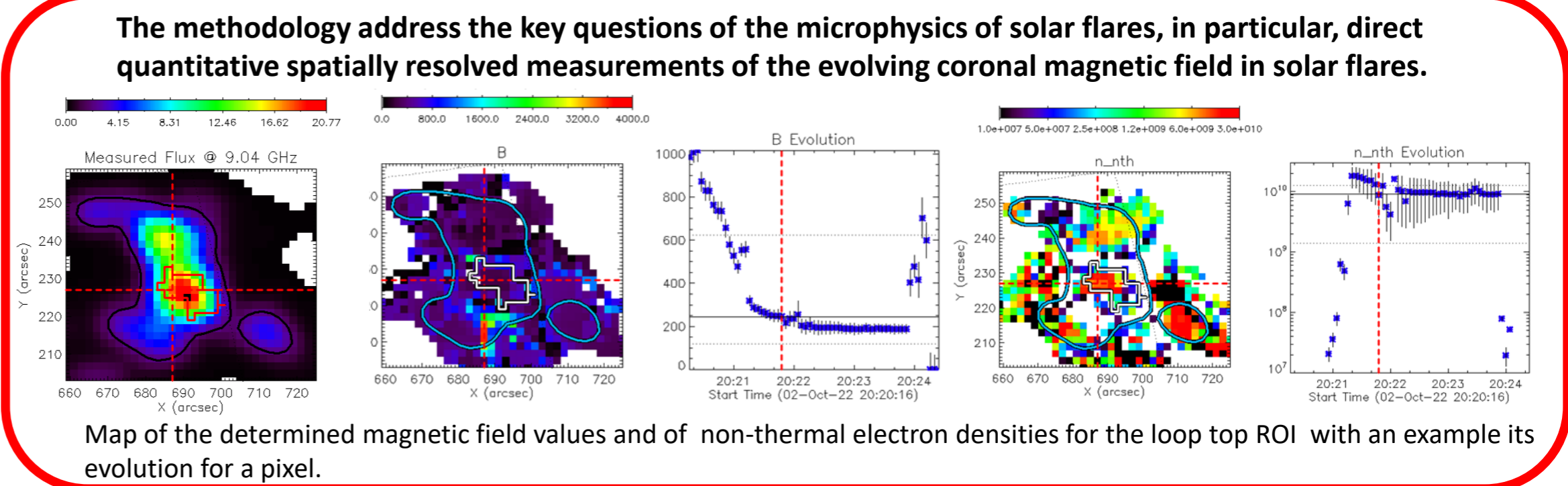
Left and center: AIA 304 Å and 211 Å images overlaid with EOVSA contours (3–18 GHz, 20% of the maximum level) and selected ROIs, including the red (top of a loop) and grey (base of the erupted filament). Right: normalized light curves of SDO/AIA.



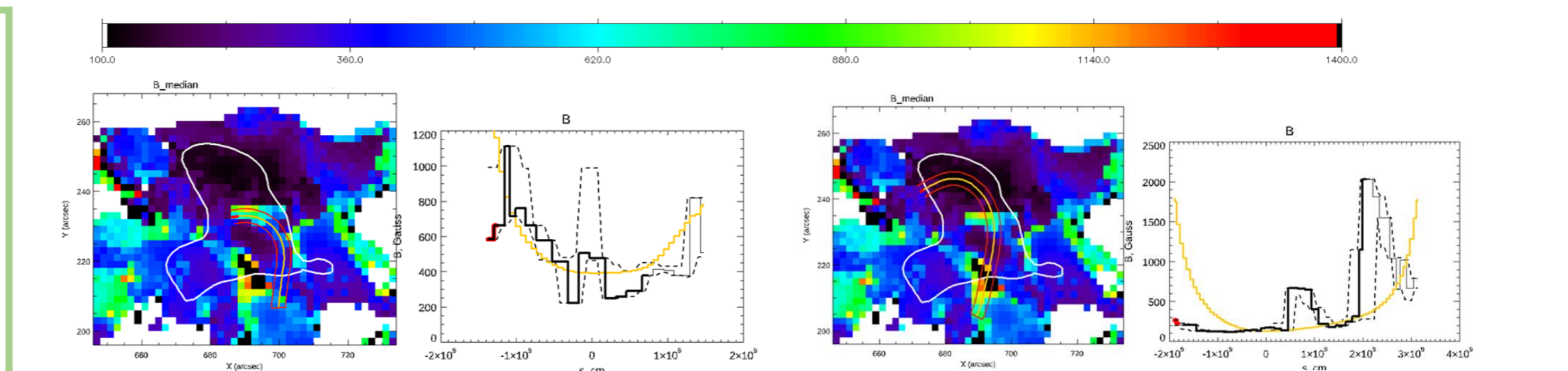
Left: AIA 335 Å. Center: AIA 1600 Å with EOVSA multispectral data. Right: EOVSA dynamic spectrum and light curve.



Left: EOVSA image on 8.71 GHz. Center: Observational and modeled spectra, along with GSFIT setting parameters in the interface of the GX Simulator (Nita et al., 2023). Right: New enhancement of fitting capabilities: example of a two-peak fit. Two peaks in the spectrum from a single pixel presumably indicate two sources projected along the line of sight. We have separated the derived parameters of these two sources into those corresponding to the upper and lower sources, respectively.



The methodology address the key questions of the microphysics of solar flares, in particular, direct quantitative spatially resolved measurements of the evolving coronal magnetic field in solar flares.



Comparison of the measured magnetic field with the results of the 3D magnetic field reconstruction based on HMI photospheric data. The background shows a map of the regularized magnetic field values for the top source obtained from a two-component fitting. The white contour represents the EOVSA emission at 8.71 GHz at 10% level. The reconstructed magnetic field lines are shown in yellow, and a 1-pixel-wide tube around these lines is indicated in red. In the adjacent images, the magnetic field values along these lines are compared. The measured values are shown by the black line, with the dashed lines indicating the uncertainties. Two examples of magnetic field lines obtained from the 3D extrapolation are presented.

Conclusions

- **Methodological Advances:** The proposed methodology addresses key questions in the microphysics of solar flares, particularly through direct quantitative spatially resolved measurements of the evolving coronal magnetic field in solar flares.
- **Magnetic Energy Release:** The locations of magnetic energy release have been identified using EOVSA microwave imaging spectroscopy data, showing good agreement with UV observational data from AIA and with coronal magnetic field reconstructions based on photosphere measurements from HMI.
- **Plasma Parameters Determined:** Detailed plasma parameters, including magnetic field strength, density, and non-thermal electron spectral indices, have been determined. For the first time, these parameters have been derived for the erupted filament at its base.
- **Magnetic Field Decay Rate:** The magnetic field decay rate at the loop top and other locations has been measured, with values reaching up to 10 G/s.

References

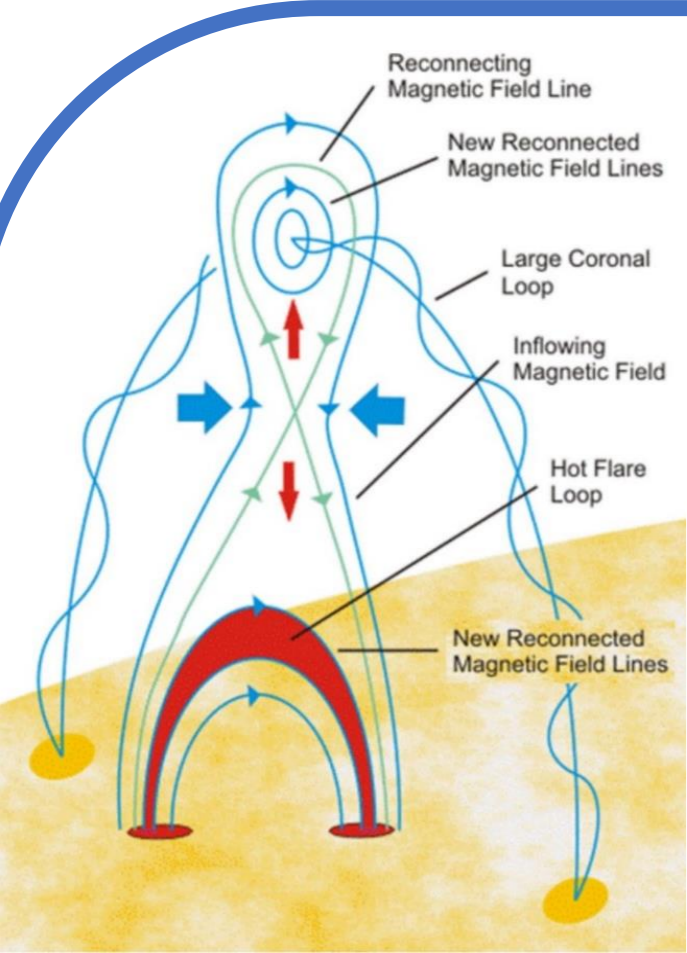
- Gary et al. 2018, Microwave and Hard X-Ray Observations of the 2017 September 10 Solar Limb Flare. *ApJ*, 863, 83,
Fleishman et al. 2020, Decay of the Coronal Magnetic Field can Release Sufficient Energy to Power a Solar Flare. *Science*, 367, 278,
Nita et al. 2023, Data-constrained solar modeling with GX Simulator. *ApJS*, 267, 6,
Song et al., 2023, Spectral Observations and Modeling of a Solar White-light Flare Observed by CHASE, *ApJL*, 952, L6,
Dai et al., 2023, Simultaneous Horizontal and Vertical Oscillation of a Quiescent Filament Observed by CHASE and SDO, *ApJ*, 959, 71.

Is the "Standard Model" valid?

- There is a **fundamental deficiency of the Standard Model**: the flare energy and other simple scaling arguments suggest that the magnetic energy is released in a **much, much larger volume** than available at/around the **X-point/current sheet**.

• **A 50-year-old Challenge in Solar Flare Physics: how, when, and where the free magnetic energy is released to drive solar flares and eruptions?**

- Because of lack of the dynamic remote probing of the coronal magnetic field in flares, until very recently, this challenge could not be addressed.



Standard Solar Flare Model

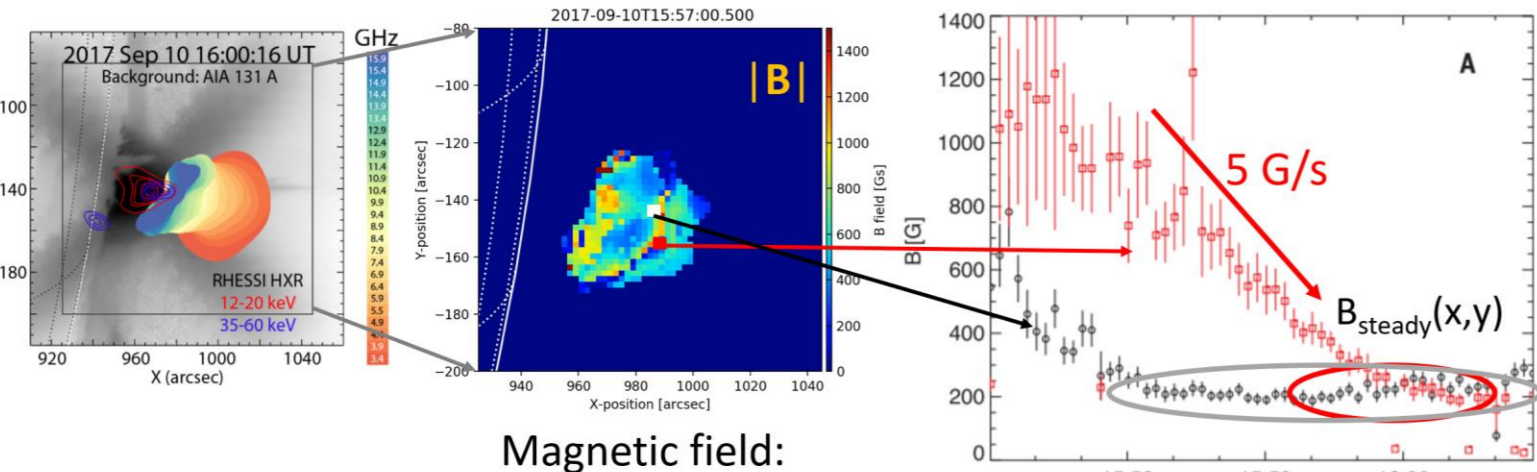
The solar corona sometimes exhibits an explosive release of the energy stored in magnetized plasma, which drives phenomena such as solar flares.

The standard model of solar flares posits that they are powered by magnetic energy stored in the solar corona and released (dissipated into other forms) through magnetic reconnection—a reconfiguration of the magnetic field topology toward a state of lower magnetic energy.

Changes in the coronal magnetic field during a flare or other large-scale eruptions have been quantified only indirectly, for example, from extrapolations of the magnetic field measured at the photosphere. The extrapolation approach does not allow the dynamic local changes of the magnetic field to be quantified at time scales short enough to characterize the flare energy release.

Microwave imaging spectroscopy data are now available from Expanded Owens Valley Solar Array (EOVSA).

B Field (0-1500 G) in 2017-Sep-10 Flare; Peak Phase



Magnetic field:

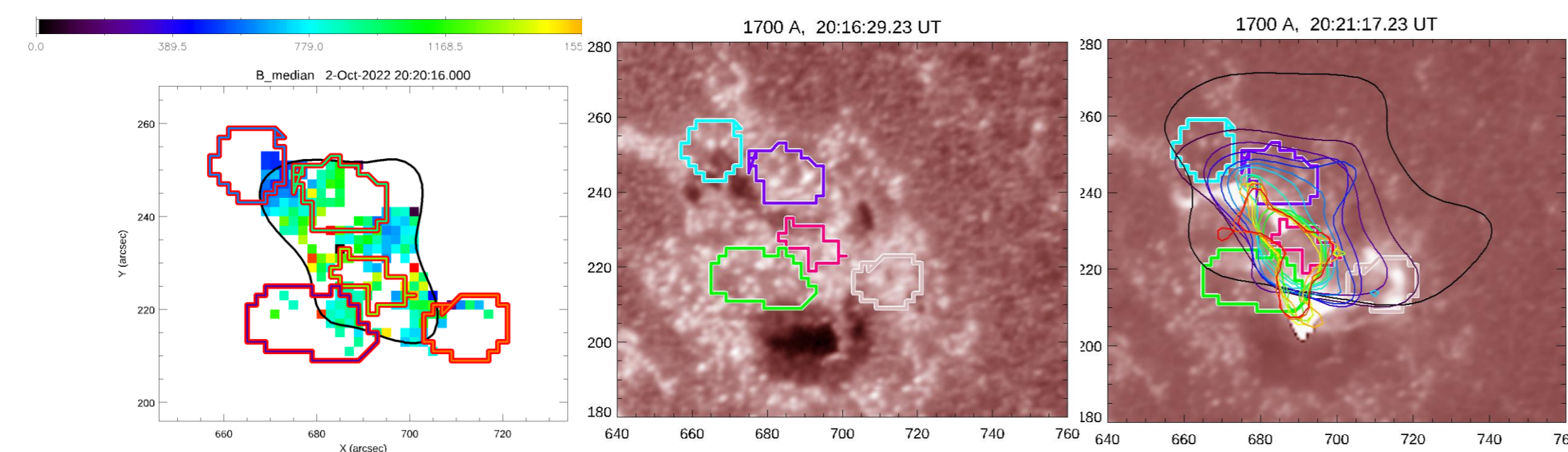
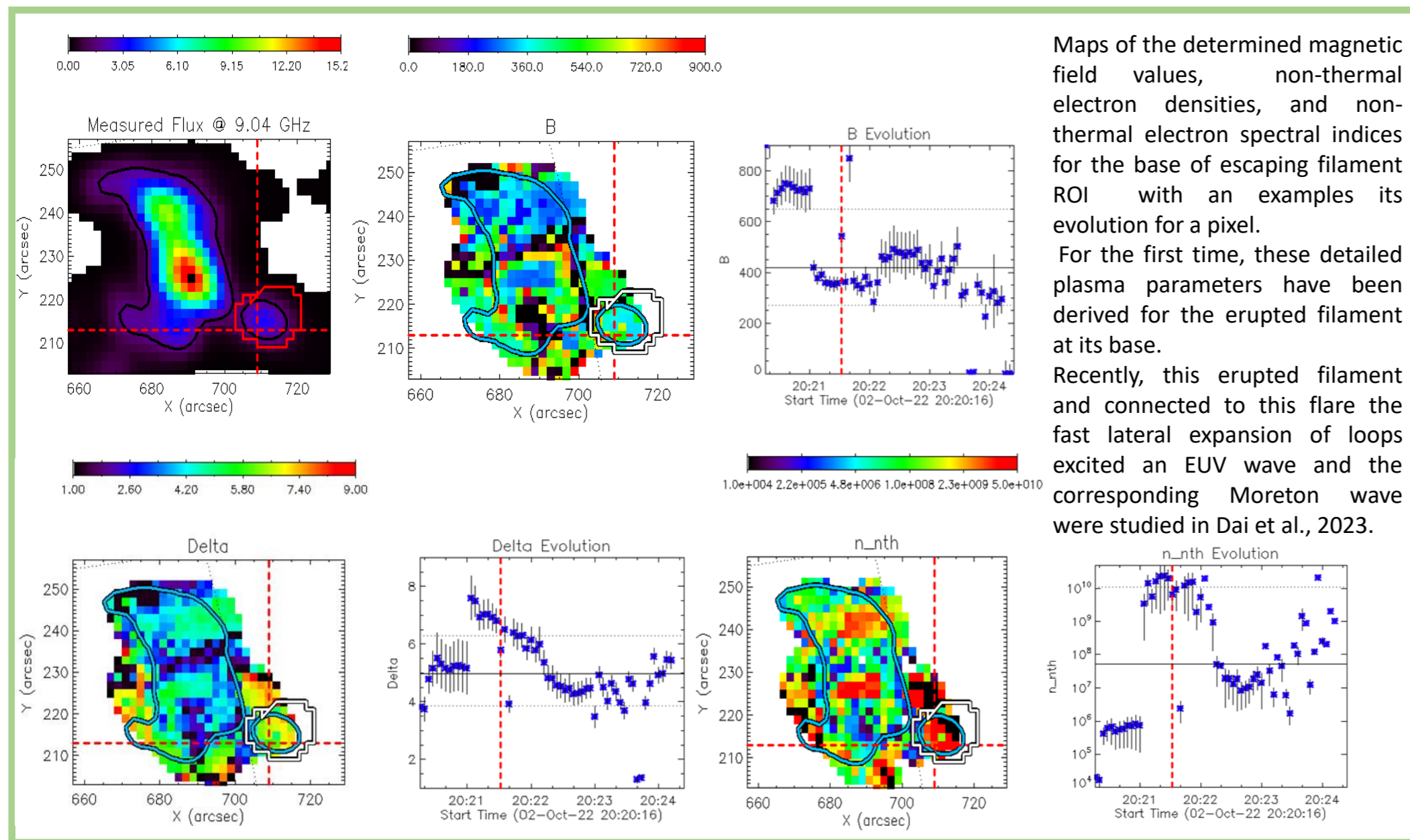
- falls with height and
- decays with time at a given height.

Fleishman et al.
Science 2020

The magnetic field decays and the magnetic energy is released **not just at the X-point** as implied by the standard model, but rather over an **EXTENDED CUSP REGION**.

Maps of the determined magnetic field values, non-thermal electron densities, and non-thermal electron spectral indices for the base of escaping filament ROI with an examples its evolution for a pixel. For the first time, these detailed plasma parameters have been derived for the erupted filament at its base. Recently, this erupted filament and connected to this flare the fast lateral expansion of loops excited an EUV wave and the corresponding Moreton wave were studied in Dai et al., 2023.

Recently, this erupted filament and connected to this flare the fast lateral expansion of loops excited an EUV wave and the corresponding Moreton wave were studied in Dai et al., 2023.



Left: Map of the regularized magnetic field values for the bottom source from two-component fitting, bounded by both a black contour representing EOVSA emission at 5.14 GHz at the 10% level and the selected ROIs.

Right: 1700 Å image (AIA/SDO) before and during the flare (the study of this white-light flare was conducted in Song et al., 2023). The flare image is overlaid with color contours of EOVSA at 20% of the maximum level. The black and red colors correspond to 3 and 18 GHz, respectively, while the other colors are distributed within this spectral range.

The complex magnetic topology and the nature of the energy release make it difficult to find an exact match between the lower microwave source and the observed brightenings in the 1600 and 1700 Å lines, but some correlation can be indicated.